

Article

DeNO_x of Nano-Catalyst of Selective Catalytic Reduction Using Active Carbon Loading MnO_x-Cu at Low Temperature

Tao Zhu ^{1,2,*}, Xing Zhang ¹, Wenjing Bian ¹, Yiwei Han ¹, Tongshen Liu ^{3,*} and Haibing Liu ⁴

¹ Institute of Atmospheric Environmental Management and Pollution Control, China University of Mining & Technology (Beijing), Beijing 100083, China; zhangxing@student.cumtb.edu.cn (X.Z.); rainbwj@outlook.com (W.B.); hanyw@student.cumtb.edu.cn (Y.H.)

² Shaanxi Key Laboratory of Lacustrine Shale Gas Accumulation and Exploitation (Under Planning), Xi'an 710065, China

³ Beijing Municipal Research Institute of Environmental Protection, Beijing 100037, China

⁴ Solid Waste Management Center of China Ministry of Ecological Environment, Beijing 100029, China; lhblff@126.com

* Correspondence: bamboozt@cumtb.edu.cn (T.Z.); ltongshen@163.com (T.L.); Tel.: +86-10-6233-9170 (T.Z.); Fax: +86-10-6233-9170 (T.Z.)

Received: 8 November 2019; Accepted: 14 January 2020; Published: 18 January 2020



Abstract: With the improvement of environmental protection standards, selective catalytic reduction (SCR) has become the mainstream technology of flue gas deNO_x. Especially, the low-temperature SCR nano-catalyst has attracted more and more attention at home and abroad because of its potential performance and economy in industrial applications. In this paper, low-temperature SCR catalysts were prepared using the activated carbon loading MnO_x-Cu. Then, the catalysts were packed into the fixed-bed stainless steel micro-reactor to evaluate the selective catalytic reduction of NO performance. The influence of reaction conditions was investigated on the catalytic reaction, including the MnO_x-Cu loading amount, calcination and reaction temperature, etc. The experimental results indicate that SCR catalysts show the highest catalytic activity for NO conversion when the calcination temperature is 350 °C, MnO_x loading amount is 5%, Cu loading amount is 3%, and reaction temperature is 200 °C. Under such conditions, the NO conversion arrives at 96.82% and the selectivity to N₂ is almost 99%. It is of great significance to investigate the influence of reaction conditions in order to provide references for industrial application.

Keywords: low-temperature SCR; activated carbon; nano-catalyst; reaction condition; NO conversion

1. Introduction

The emission of nitrogen oxides (NO_x) has aroused widespread concern in recent years, which is dangerous to human health and brings many negative effects on the environment, such as urban smog, acid rain, and so on. Increasingly stringent limits for flue gas emissions have driven many researchers to look for suitable methods [1,2]. Selective non-catalytic reduction (SNCR) is a more economical NO_x control method with a considerable efficiency of 40–70%, which involves the reduction of NO_x by a nitrogen agent, usually ammonia (NH₃) or urea, and it is relatively simple to implement. Although reasonably inexpensive, SNCR process has a serious limitation. For example, the NO_x reduction efficiency drops off drastically at slightly higher or lower temperatures because the temperature window over which nitrogen agents are effective is relatively narrow [3,4]. The selective catalytic reduction (SCR) of NO_x with NH₃ has been regarded as the most effective method to reduce the emission of NO_x. However, the SCR catalysts have to be placed upstream of the electrostatic

precipitator and desulfurization units to avoid costly heating of the flue gas due to its high working temperature window (300–400 °C), where the SCR catalysts are susceptible to deactivation by dust accumulation and sulfur poison. As an alternative, low-temperature SCR catalysts could be placed downstream of the electrostatic precipitator and desulfurization units. Therefore, it is crucial to develop low-temperature SCR catalysts, which can work at 200 °C or even lower, and adapt to the complex flue gas environment [5–7]. Many scientists whether foreign and domestic had carried out the study of low-temperature SCR catalysts and their main research contents included the active component and catalyst support. However, sintering often occurs in the preparation of single component SCR catalyst, which reduces the dispersion of the active component and the activity of the SCR catalyst. The sintering is avoided by adding transition metal and the performance of SCR catalyst is improved. Therefore, the researches and developments of low-temperature SCR catalyst focused on the transition metal oxide catalyst at home and abroad [8–11]. Copper and copper compounds are thought to have excellent catalytic properties at low temperatures, which can improve the physical properties of the SCR catalyst as a promoter [12,13]. Chmielarz et al. prepared a M-Mg-Al catalyst with a coprecipitation of hydrotalcite (M=Cu²⁺, Co²⁺, and Cu²⁺+Co²⁺), and they compared the catalytic properties of the mixed catalyst. The results showed Cu-Mg-Al > Cu-Co-Mg-Al > Co-Mg-Al and the deNO_x efficiency of 80–95% at temperatures of 200–250 °C [14].

Manganese (Mn) is thought to have a very outstanding catalytic property at low temperatures, and Mn-based catalyst has been widely studied over the past few decades owing to its low cost. In relation to the supported metal oxide catalysts, the researchers mainly focused on the MnO_x catalyst. MnO_x is characterized by strong catalytic performance for NO_x as the active component of the SCR catalyst. There are many kinds of MnO_x due to the wide distribution of the Mn valence. The Mn with a different valence can be converted to each other, which promotes the selective reduction of NO_x by NH₃. Therefore, the valence state of Mn in MnO_x has a significant effect on the activity of the SCR catalyst. Moreover, composite oxide catalysts are of great interest because one metal element can modify the catalytic properties of another, which results from both electronic and structural influences. For example, binary metal oxide solid solutions might be formed between Mn and Cu [15,16]. Qi et al. used a different precipitation agent to prepare a series of Mn oxide catalyst by coprecipitation, and the catalyst activities were investigated under the condition of NH₃-NO_x. The results indicated that the catalyst was of high catalytic activity at a low temperature using sodium carbonate as a precipitant preparation of Mn oxide catalysts [17]. Ouzzine et al. studied the Mn-Cu composite catalyst and found that the catalytic temperature range was wide through the activity test. The NO_x conversion was more than 60% in the range of 150–400 °C. What is more, they found that Cu could absorb sulfur dioxide and form sulfate, which improved sulfur resistance greatly [18]. Yao et al. successfully prepared a series of Mn/CeO₂ catalysts via impregnation using deionized water, anhydrous ethanol, acetic acid, and oxalic acid as a solvent and found that the Mn/Ce catalyst exhibited the best water and sulfur tolerance [19]. Therefore, mixing MnO_x with suitable metal oxides and loading Mn-based active components on a suitable support could be considered as an efficient strategy [20].

Activated carbon (AC) is a kind of materials with a high specific surface area, unique pore structure, excellent dispersion of active components and chemical stability, which has been widely studied as substrates for supporting low-temperature SCR catalysts. If AC is adopted as the catalyst support, the possibility of sintering deactivation could be reduced [21–25]. Valdés-Sols et al. confirmed that the vanadium loaded on the carbon-ceramic body was of a good low-temperature property, and the ability to resist the poison of catalyst for sulfur dioxide was greater than the Mn catalyst. But water vapor in the flue gas had an influence on the catalyst activation [26]. García-bordejé et al. studied low-temperature SCR characteristics using carbon materials loaded on a honeycomb support, and vanadium loaded on the carbon material. They found that deNO_x efficiency was 59.8–72.1% at 150 °C and 68–78.6% at 180 °C [27]. Shanxi Institute of Coal Chemistry of Chinese Academy of Sciences prepared a SCR catalyst of V₂O₅ loaded on the carbon honeycomb support. They found the catalyst

not only had a deNO_x effect, but also could resist SO₂ poisoning. But the engineering practicability of the low-temperature SCR catalyst still needs further research [28,29].

Although the catalyst varied, it is the key problem on how to effectively reduce NO_x emission from flue gas at a low temperature and with low energy. At the same time, the SCR catalysts in industrial application are facing many problems, such as high costs, poisoning and transformations. The steady increase of NO_x emissions necessitates the improvement of abatement technologies [30]. In this context, the research on low-temperature SCR catalyst was launched. According to the data, 95% of NO_x in flue gas is in the form of NO. The by-products NO₂ and N₂O were formed in the reaction, but the amount generated was very small. Therefore, NO was used to simulate the catalytic reduction of NO_x in this research and the NO conversion was taken as an index of the SCR catalyst [31,32]. The influence of reaction conditions on NO conversion was investigated, including the MnO_x-Cu loading amount, calcination and reaction temperatures, etc. The optimal preparation and reaction conditions of low-temperature SCR catalyst were determined in a series of experiments so that it could provide basic research data for industrial application.

2. Results and Discussion

2.1. The Characterization of Support

The AC was purified by 1%, 5% and 10% nitric acid, then filtered, washed and dried, respectively. Observed by the X-ray diffraction (XRD) pattern as shown in Figure 1, there are two dispersed peaks in the scope from 20 to 30°, and there are three dispersed peaks in the scope from 30 to 40°. The skeleton structure of AC is similar to amorphous carbon and it is mainly composed of graphite microcrystals in which 2–4 layers single layer graphite sheets are stacked. The dispersed peaks are graphite microcrystals with different structures, which indicates that the AC sample has a low graphitization structure and silica is an inorganic component of AC. There is almost no amorphous peak in the XRD diffraction pattern of the AC, which indicates that AC is of good crystallinity after processing.

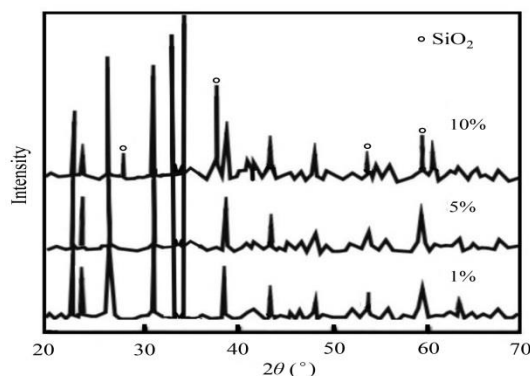


Figure 1. XRD pattern of AC.

The Brunauer-Emmett-Teller (BET) surface areas, pore volumes and pore sizes of AC are summarized in Table 1. From Table 1, the BET surface area of AC increases by about 9.10% after the nitric acid purification process, and total pore volume is not significant. It is worth noting that the purified micropore volume of AC increases and the average pore diameter decreases. Obviously, the nitric acid process enhances the microporous nature of AC, which is conducive to the dispersion of MnO_x and Cu on the AC surface. Furthermore, it is beneficial for SCR catalyst in terms of mass transfer, adsorption and activation of reactants during the reaction [33]. The AC average pore diameter falls in the range of 8–11 nm, favoring gas molecule diffusion in the pores and thus ruling out the diffusion limitation in the adsorption and desorption process.

Table 1. Physical characteristics of AC.

Sample	BET Surface Area (m ² /g)	Total Pore Volume (cm ³ /g)	Micropore Volume (cm ³ /g)	Average Pore Diameter (nm)
Before processing	638 ± 1.96	0.29 ± 0.01	0.26 ± 0.02	10.27 ± 0.03
After processing	696 ± 2.28	0.30 ± 0.02	0.31 ± 0.03	8.56 ± 0.02

2.2. The Influence of MnO_x Loading Amount on Catalytic Activity

The influence of MnO_x loading amount on SCR catalyst activity was investigated when the Cu loading amount (% wt) was 1%, 3%, 5%, 7%, 10%, respectively. The calcination temperature was 350 °C. The experiments compared the different MnO_x loading amount of SCR catalyst under different reaction temperatures for NO conversion. Figure 2 presents the NO conversion changes with MnO_x loading amounts and reaction temperatures when Cu loading amounts were 1%, 3%, 5%, 7%, 10%, respectively.

When MnO_x loading amounts change in the scope of 1–5%, NO conversion increases with the increase of MnO_x loading amounts. There are more active sites if the catalyst has more active components, which is helpful to enhance catalytic activity. However, NO conversion decreases when MnO_x loading amounts change in the scope of 5–10%. All the experimental results indicate that SCR catalysts show optimal performance when the MnO_x loading amount reaches 5%, and NO conversion arrives at 95.31%, 96.82%, 95.20%, 92.65%, 88.00% at a reaction temperature of 200 °C. As can be seen from Figure 2, the SCR catalyst shows strong activity at 200 °C, which indicates that the SCR catalyst is suitable for deNO_x of low temperature flue gas. Whatever the Cu loading amount change, NO conversion reaches the maximum with a MnO_x loading amount of 5%, and the N₂ selectivity remains stable at nearly 99%.

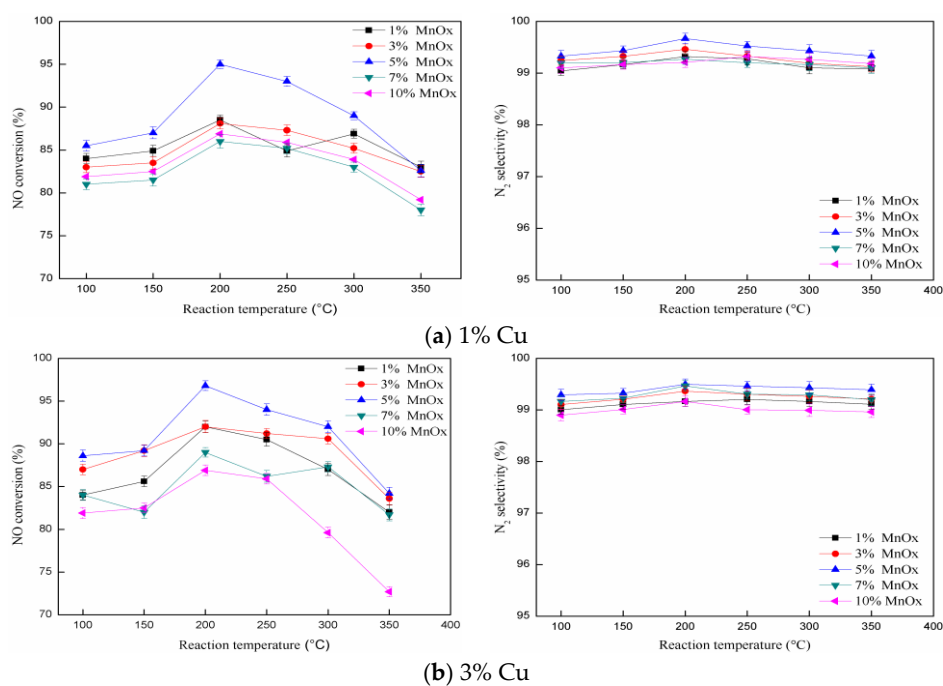


Figure 2. Cont.

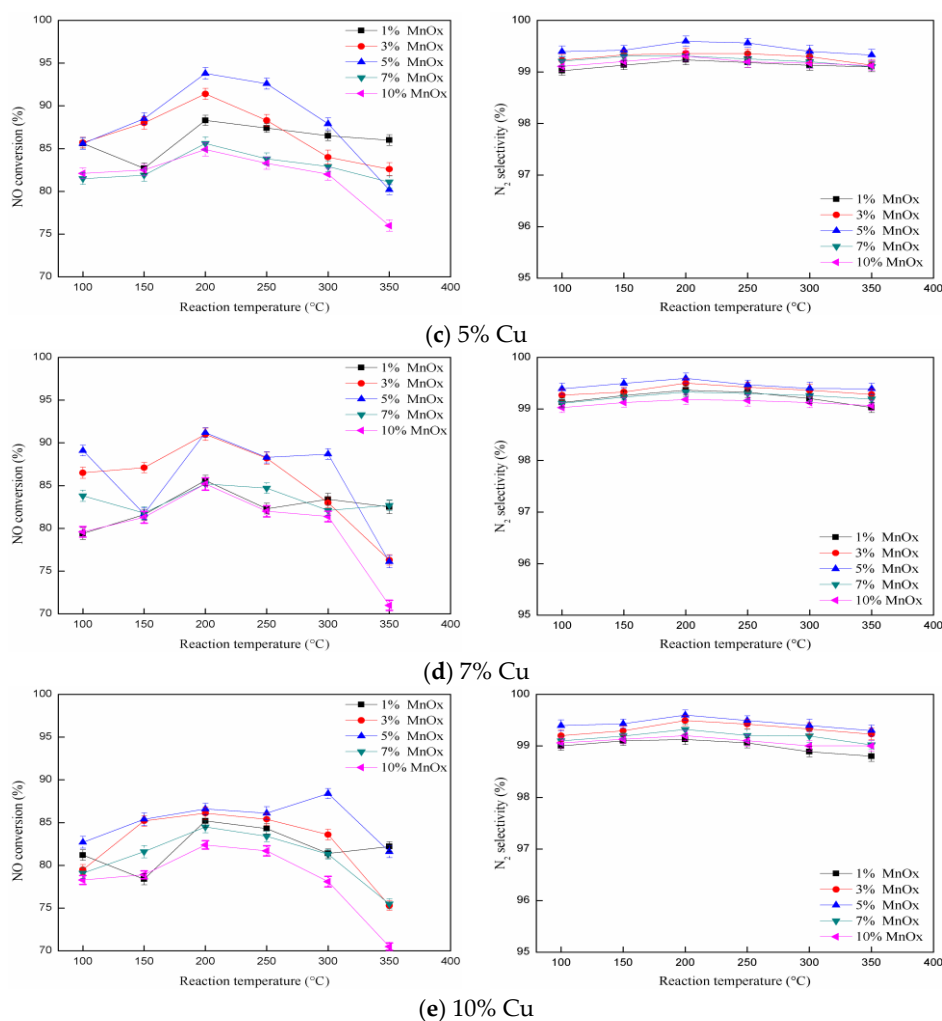


Figure 2. Relationship between MnO_x loading amount and NO conversion with a Cu loading amount of (a) 1%, (b) 3%, (c) 5%, (d) 7%, (e) 10%, respectively.

2.3. The Influence of Cu Loading Amount on Catalytic Activity

The influence of Cu loading amount on SCR catalyst activity was explored when MnO_x loading amounts (% wt) were 1%, 3%, 5%, 7%, 10%, respectively. The calcination temperature was 350 °C. The experiments compared the different Cu loading amount of the SCR catalyst under different reaction temperatures for NO conversion. Figure 3 illustrates the influence of the Cu loading amount on NO conversion with different MnO_x loading amounts. NO conversion arrives at 93.58%, 93.79%, 96.82%, 91.82%, 87.93% when the Cu loading amount is 3%, and the reaction temperature is 200 °C, respectively.

When the Cu loading amount changes in the scope of 1–3%, NO conversion always increases with the increase of the Cu loading amount. However, NO conversion decreases when the Cu loading amount changes in the scope of 3–10%. Whatever the MnO_x loading amount changes, NO conversion reaches the maximum with a Cu loading amount of 3%, and the N₂ selectivity remains stable at nearly 99%. On the whole, NO conversion decreases gradually when the reaction temperature exceeds 200 °C. This result reveals that the MnO_x-Cu/AC catalyst has a good activity at a low temperature.

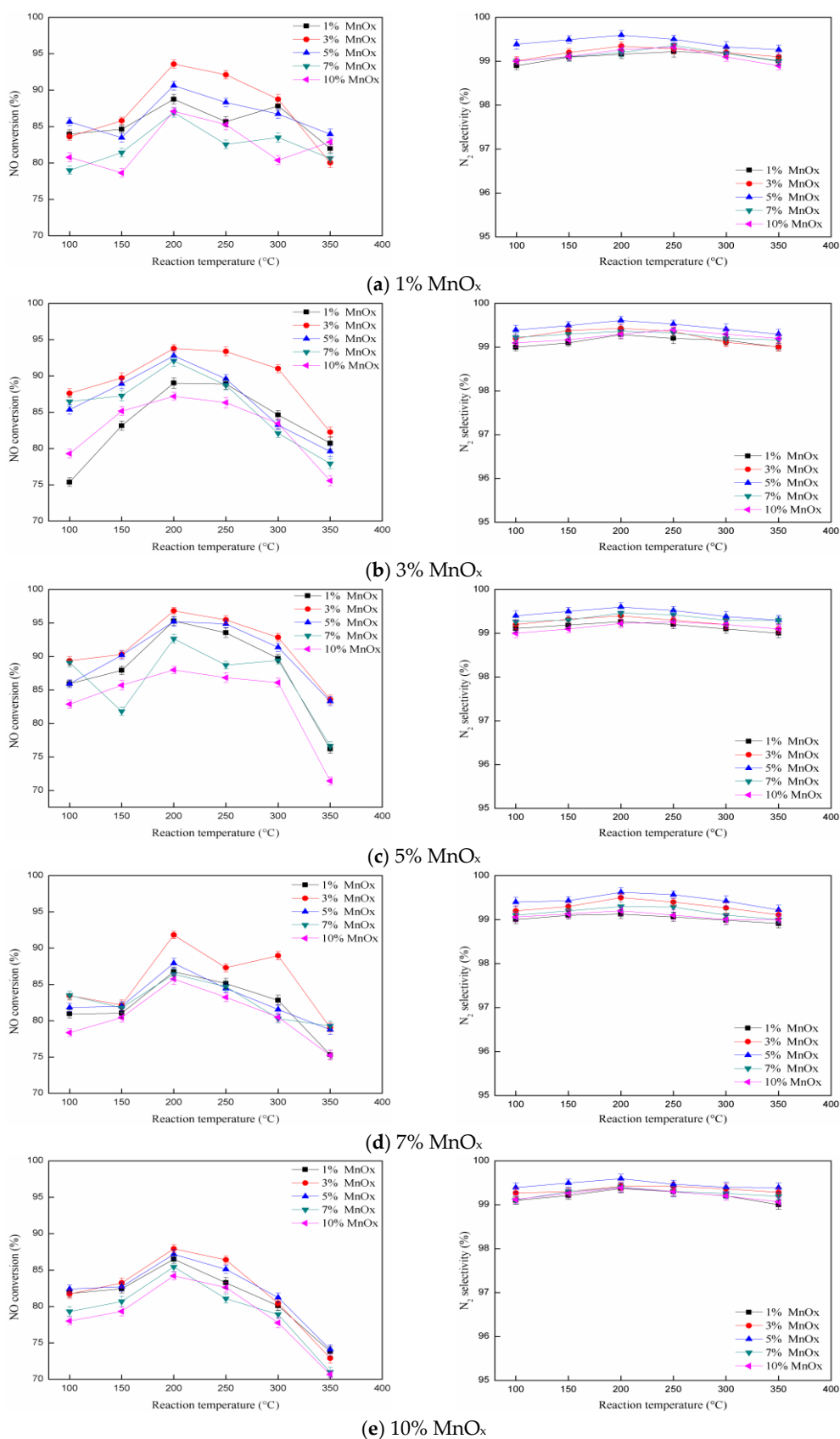


Figure 3. Relationship between the Cu loading amount and NO conversion with the MnO_x loading amount of (a) 1%, (b) 3%, (c) 5%, (d) 7%, (e) 10%, respectively.

2.4. The Influence of Calcination Temperature on Catalytic Activity

In four different calcination temperatures (250 °C, 300 °C, 350 °C and 400 °C), the SCR catalysts (Cu loading amount of 3%, and MnO_x loading amount of 5%) were prepared. Figure 4 shows that NO conversion is highest up to 96.49% when the calcination temperature is 350 °C, and the N₂ selectivity remains stable at nearly 99%.

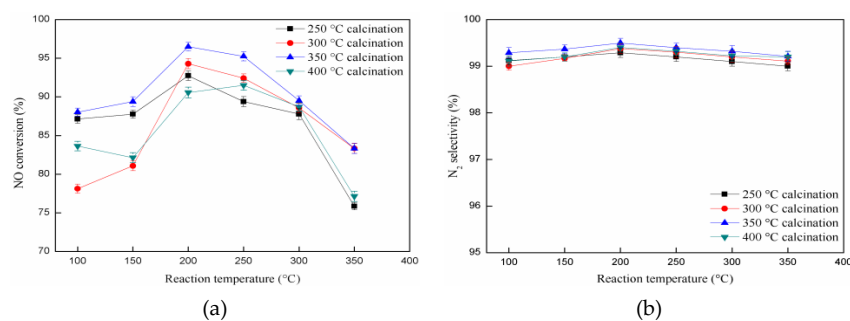


Figure 4. The influence of calcination temperature on catalytic activity. (a) NO conversion; (b) N₂ selectivity.

The SCR catalyst could not give full play to the function because MnO_x and Cu might not integrate adequately due to the calcination temperature of 300 °C. When the calcination temperature reaches 400 °C, the temperature may lead to the inside pore channels of SCR catalyst to be collapsed or closed due to sintering, which reduces the number of active sites on the surface of the SCR catalyst. The high calcination temperature may reduce the dispersion of active sites [34]. Huang et al. found that the suitable calcination temperature could improve the attrition strength of the SCR catalyst, while the continuous increase of the calcination temperature could change the mechanical property and catalytic performance of the SCR catalyst in a perverse way [35].

2.5. The Influence of Reaction Temperature on Catalytic Activity

From the above experiments, NO conversion reaches a maximum at a calcination temperature of 350 °C, MnO_x loading amount of 5%, and Cu loading amount of 3%. Then the MnO_x-Cu/AC catalysts were prepared under that condition. The influence of reaction temperature on NO conversion was investigated at 100 °C, 150 °C, 200 °C, 250 °C, 300 °C, 350 °C, respectively.

Figure 5 presents that the NO conversion of MnO_x-Cu catalyst increases firstly and then decreases with the increase in reaction temperature, and the N₂ selectivity remains stable at nearly 99%. Especially, the NO conversion reaches 96.82% when the reaction temperature is 200 °C. According to Ren's research, the reason why NO conversion increases rapidly with the increase in temperature is that the consumption of NH₃ is mainly for the NO reduction reaction. Therefore, NO conversion increases rapidly in the temperature range of 100 to 200 °C. After that, NO reaction will be restricted for the occurrence of NH₃ oxidation reaction if the reaction temperature continues to rise, that is because the NH₃ oxidation reaction will easily occur at a high reaction temperature [36].

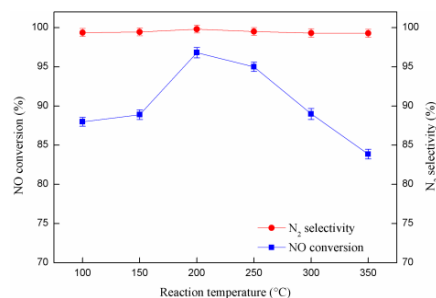


Figure 5. The influence of reaction temperature on catalytic activity.

2.6. The Catalytic Stability Test of SCR Catalyst

Long-time stability is a crucial indicator to evaluate the catalytic performance of SCR catalysts in practical industrial application. As shown in Figure 6, a 25 h stability test was carried out to investigate catalytic stability at 200 °C. The calcination temperature of the MnO_x-Cu/AC catalyst was 350 °C. Throughout the 25 h continuous procedure, the deNO_x activity of MnO_x-Cu/AC catalyst is rather stable with a slight fluctuation around ±1% over time, the NO conversion remains at nearly 96%, and the selectivity of N₂ is almost 99%. There is almost no deactivation occurring during 25 h at 200 °C, which further demonstrates that the MnO_x-Cu/AC catalyst behaves with excellent stability.

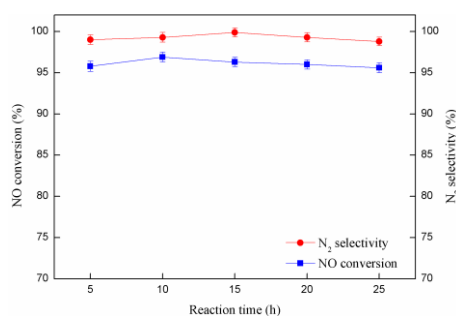


Figure 6. The catalytic stability of the SCR catalyst with the loading amount of 5% MnO_x and 3% Cu.

2.7. The Catalytic Activity Analysis of the SCR Catalyst

In order to explore the relationship between the structure and performance in detail, microstructure and micromorphology analysis were performed. The XRD pattern of SCR catalysts with a loading amount of 3%, 5% MnO_x and 3%, 5% Cu is shown in Figure 7, which presents that the obvious peaks are between 20° and 50°. Its main phase is graphite microcrystal with different structures. The MnO_x is not found in the XRD pattern, which is consistent with Jiang's report and indicates that the active component is present in an amorphous state. Moreover, it is very likely that Mnⁿ⁺ ions are incorporated into the copper oxide lattice to form a solid solution during the calcinations [37]. The amorphous MnO_x may be one of the key factors for the excellent catalytic activity in deNO_x performance according to Tang's research [38]. CuO shows a peak at 37.2°, and Wang et al. found that Cu was present nearly exclusively in the form of mononuclear ions and oligomeric species [39].

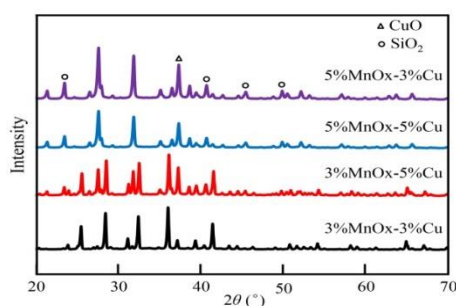


Figure 7. The XRD pattern of SCR catalysts with the loading amount of 3%, 5% MnO_x and 3%, 5% Cu, respectively.

XPS analysis was carried out to determine the atomic concentration and chemical states of different species presented on catalysts surface. Figure 8 shows the oxidation state of Mn species and the binding energy peaks of Mn 2p for MnO_x/Cu-AC catalyst. The Mn 2P_{3/2} peak of 5% MnO_x-3% Cu/AC catalyst can be separated into three peaks, i.e., 642.3 eV, 643.4 eV and 644.7 eV, which correspond to Mn²⁺ species, Mn³⁺ species and Mn⁴⁺ species, respectively. The active components are mainly in the form of MnO, Mn₂O₃ and MnO₂. The Mn valence binding energy distribution of SCR catalysts as

shown in Table 2, and the valence distribution of Mn oxides are dominated by Mn^{3+} and Mn^{4+} . The MnO_x catalytic activity has been ascribed to the potential of Mn to form several oxides and to provide oxygen selectively from its crystalline lattice [40]. The proportion of Mn^{3+} and Mn^{4+} reaches maximum when the loading amount of Cu is 3%, which indicates that the reducibility of the SCR catalyst is relatively strong. Xin et al. suggested that Mn^{3+} could activate NH_3 into NH_2 intermediate that would readily react with NO to produce N_2 [41]. Yao et al. confirmed that an ample amount of Mn^{4+} ions is one of the key factors enhancing NH_3 oxidation in the NH_3 -SCR process due to the strong oxidizing state of Mn (IV) [42]. According to Lee's research, the existence of various Mn valences increased the electron transfer during the NO conversion processes, which could promote the denitration reaction for NH_3 -SCR [43]. Fang et al. found that there was a strong interaction between manganese oxides and copper oxides, and the valence distribution of Mn was affected by the loading amount of Cu [44]. Furthermore, a synergistic interaction between Mn and Cu might exist according to the redox couple: $\text{Mn}^{3+} + \text{Cu}^{2+} \rightarrow \text{Mn}^{4+} + \text{Cu}^+$.

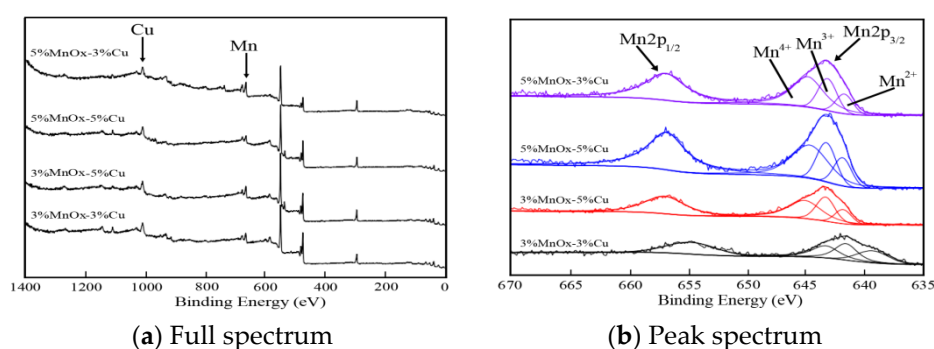


Figure 8. The XPS pattern of SCR catalysts with the loading amount of 3%, 5% MnO_x and 3%, 5% Cu, respectively. (a) Full spectrum; (b) Peak spectrum.

Table 2. The Mn valence binding energy distribution of SCR catalysts.

SCR Catalysts	Mn^{2+} (eV)	Mn^{3+} (eV)	Mn^{4+} (eV)	$\text{N}(\text{Mn}^{3+} + \text{Mn}^{4+})/\text{n}(\text{Mn}^{x+})$
5% MnO_x -3% Cu	642.3	643.4	644.7	0.86
5% MnO_x -5% Cu	642.3	643.4	644.8	0.85
3% MnO_x -5% Cu	642.1	643.2	644.8	0.82
3% MnO_x -3% Cu	640.2	641.8	643.5	0.78

The distribution of acidic sites were characterized by NH_3 -TPD with the loading amount of 3%, 5% MnO_x and 3%, 5% Cu, respectively. The calcination temperature was 350 °C. As is shown in Figure 9a, the weaker desorption peak appears at 68 °C, which corresponds to the weak acidic sites of SCR catalysts. In addition, the stronger desorption peak appears at 142 °C, which corresponds to the strong acidic sites. The peak area and intensity of the catalyst with a loading amount of 5% MnO_x -3% Cu are higher than others, which indicates that there are more acidic sites in the catalyst surface. The optimum combination ratio makes the active component of MnO_x dispersed uniformly, and it is conducive to improving the activity of the SCR catalyst [45]. Many research showed that surface acidity played a critical role in SCR reaction [46,47]. Therefore, the increased acidic sites might represent one of the most important reasons for the higher catalytic activity of the MnO_x -Cu/AC catalyst. Yao et al. found that the synergistic effects between Mn and Cu ions could further enhance the low-temperature performances via modified active sites [48]. Moreover, Shu et al. found that surface acidity played a critical role in the SCR reaction [49]. Consequently, the increased acidic sites might represent one of the most important reasons for the higher catalytic activity of the MnO_x -Cu/AC catalyst.

The redox property is an important index to evaluate the performance of catalysts, and H_2 -TPR technology provides an effective way in measuring the reducibility of the SCR catalyst. The sample amount of SCR catalyst was 0.10 g and the concentration of H_2 was 3% in the process of analysis.

Figure 9b presents the TPR profiles of the $\text{MnO}_x\text{-Cu/AC}$ catalyst, and the H_2 consumption amounts in the temperature range of 100–220 °C are summarized in Table 3. As can be seen from Figure 9b, one reduction peak is observed for $\text{MnO}_x\text{-Cu/AC}$ catalyst, which can be attributed to the reduction of MnO_x , and the peak area of 5% of the $\text{MnO}_x\text{-3% Cu/AC}$ catalyst is higher than others. The reduction peak appears around 200 °C, and the reduction of $\text{MnO}_2 \rightarrow \text{Mn}_2\text{O}_3 \rightarrow \text{MnO}$ may occur at this process [50,51]. The TPR profiles of the $\text{MnO}_x\text{-Cu/AC}$ catalyst are able to deconvoluted into three Gaussian peaks (dotted curves). The lowest temperature peak (150–177 °C) is attributed to the reduction of highly dispersed MnO_x surface species, the higher temperature peak (194–208 °C) corresponds to the bulk-like MnO_x , and the highest temperature peak (200–212 °C) appearing in the $\text{MnO}_x\text{-Cu/AC}$ catalyst is related to the MnO_x strongly interacted with CuO [52,53]. It could be concluded that H_2 consumption amounts increase with the increase of the Mn and Cu loading amount, and the H_2 consumption of 5% of the $\text{MnO}_x\text{-3% Cu/AC}$ catalyst is obviously higher than that of others, which suggests that the reducibility is relatively strong and verifies that 5% $\text{MnO}_x\text{-3% Cu}$ is the optimal ratio. Dong et al. found that Cu and Mn elements might form the copper galaxite of CuMn_2O_4 , and the interaction between MnO_x and Cu improved the activity of the catalyst effectively and was beneficial for NO conversion [54].

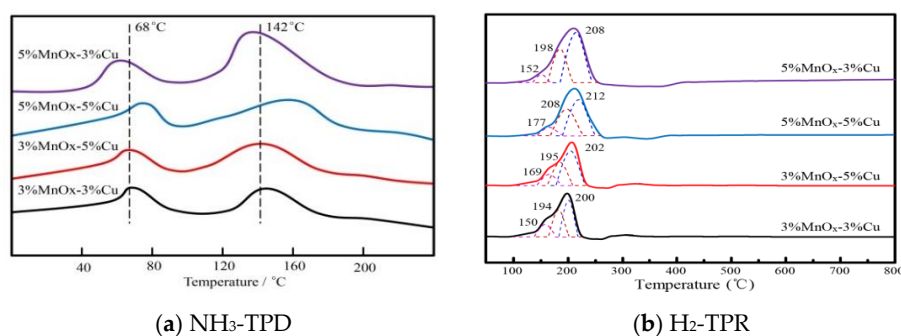


Figure 9. The acid and redox properties of the SCR catalysts with the loading amount of 3%, 5% MnO_x and 3%, 5% Cu, respectively. (a) $\text{NH}_3\text{-TPD}$; (b) $\text{H}_2\text{-TPR}$.

Table 3. The H_2 consumption of the SCR catalysts.

SCR Catalysts	Peak Area	H_2 Consumption ($\mu\text{mol/g}$)
5% $\text{MnO}_x\text{-3% Cu}$	7197	828
5% $\text{MnO}_x\text{-5% Cu}$	6883	791
3% $\text{MnO}_x\text{-5% Cu}$	6790	780
3% $\text{MnO}_x\text{-3% Cu}$	6612	759

2.8. The Reaction Mechanism of $\text{NH}_3\text{-SCR}$

According to the above research, the optimal component ratio of the SCR catalyst is loaded 5% MnO_x and 3% Cu on AC. The large specific surface area of AC is beneficial to the uniform loading of active component Mn. NH_3 and NO simulate the catalytic reduction in this work. As for the reaction mechanism of SCR, more and more scholars think that the SCR catalytic reaction should comply with the Eley-Rideal (E-R) mechanism. Another view with the Langmuir-Hinshelwood (L-H) mechanism is now accepted for the $\text{NH}_3\text{-SCR}$ process reaction mechanism. For the E-R mechanism, the redox reaction takes place between active NH_3 and gaseous NO. The adsorbed NH_3 is activated at the weak acid site on the surface of the catalyst, with the adsorption and activation of NH_3 as the critical step. For the L-H mechanism, the NO of the gas phase first interacts with O_2 and subsequently the NO_x is adsorbed onto the surface of the catalyst where it is oxidized to nitrates and nitrites in the role of lattice oxygen [55–59]. The NO removal mechanism of the $\text{MnO}_x\text{-Cu/AC}$ catalyst can be seen in Figure 10. In both E-R and L-H catalytic mechanisms, acidic sites are beneficial to the adsorption and activation of NH_3 and NO_x in a low-temperature $\text{NH}_3\text{-SCR}$ process [60–62]. Kijlstra et al. suggested that the Mn^{3+}

location on the surface of $\text{MnO}_x/\text{Al}_2\text{O}_3$ was the Lewis acid center [63]. On the $\text{MnO}_x\text{-Cu}$ catalysts, a mechanism similar with that on the $\text{MnO}_x/\text{Al}_2\text{O}_3$ were pointed out by researchers. Most researchers believe that NH_3 is adsorbed to the Lewis acid center and intermediates like NH_2^* or adsorbed NH_3 formed, then they react with NO through the E-R mechanism getting N_2 and H_2O [64,65]. Yang et al. found that chemisorption mechanism was responsible for the adsorption of reactants through density functional theory calculations and NH_2^* produced from NH_3 dehydrogenation was identified as a key reactive intermediate in the selective catalytic reduction activity of NO with NH_3 over CuMn_2O_4 spinel [66]. For the catalytic process, the optimal reaction pathway of N_2 formation in $\text{NH}_3\text{-SCR}$ of NO is a two-step process: (1) NH_2 formation from NH_3 dehydrogenation ($\text{NH}_3^* + * \rightarrow \text{NH}_2^* + \text{H}^*$), and (2) the reaction between NH_2 and NO ($\text{NH}_2^* + \text{NO}^* \rightarrow \text{N}_2^* + \text{H}_2\text{O}^*$).



Figure 10. NO removal mechanism of the $\text{MnO}_x\text{-Cu/AC}$ catalyst.

3. Materials and Methods

3.1. Catalyst Preparation

AC was used as the support to prepare the low-temperature SCR catalysts in this experiment, which was purchased from Sinopharm Chemical Reagent Ltd Co. Twenty mesh beforehand and smaller AC particles were selected in order to ensure the uniform particle size of AC. The original AC contained many impurities, such as amorphous carbon and Fe, Ni and Co, etc. Therefore, it was necessary to purify AC to avoid the influence of these impurities on catalyst preparation. Firstly, AC particles were added to different concentrations of nitric acid in turn and stirred for 2 h. Next, these activated carbon particles experienced dilution, filtering, deionized water flushing to $\text{pH} = 6\text{--}7$ in turn. Then, $110\text{ }^\circ\text{C}$ drying in electrothermal blowing for 12 h. The AC was supported with MnO_x and Cu using impregnation methods, where Mn and Cu nitrates were dissolved in deionized water, and a certain amount of the AC was added. The mixture of metal nitrates and carbon was heated and continuously stirred for 5 h after impregnated with a rotary evaporation instrument for 2 h, and then these particles were dried respectively in $110\text{ }^\circ\text{C}$ for 5 h and in $50\text{ }^\circ\text{C}$ for 12 h. After drying, the sample was calcined in a certain temperature under N_2 atmosphere for 2 h. Finally, the sample was cooled down to room temperature with protection of N_2 , and the $\text{MnO}_x\text{-Cu/AC}$ catalyst was packed into a fixed-bed stainless steel micro-reactor for the performance evaluation of SCR for NO conversion.

3.2. Catalyst Characterization

X-ray diffraction (XRD) measurement was performed by an XRD-7000 S system (Shimadzu Corporation, Japan). The 2θ scans covered the range from 10° to 80° at a 5° min^{-1} scan rate and a step of 0.02° . Cu $K\alpha$ radiation was employed, and the X-ray tube was operated at 40 kV and 40 mA. Specific surface area and pore size were calculated by the Brunauer-Emmett-Teller (BET) method and the Barrett-Joyner-Halenda (BJH) method, respectively. The surface atomic states of the catalysts were analyzed by X-ray photoelectron spectroscopy (XPS, AXIS Ultra DLD) with Al $K\alpha$ radiation ($h\nu = 1486.6 \text{ eV}$) as the excitation source at 150 W. C1 s-binding energy of 284.6 eV was taken as a reference. The hydrogen temperature programmed reduction (H_2 -TPR) experiments of the prepared catalysts were performed on a Tianjin XQ TP5080 auto-adsorption apparatus. Prior to the H_2 -TPR experiment, 0.10 g of the catalyst was pretreated with Ar at a total flow rate of 50 mL/min at 200°C for 1 h, and subsequently cooled to room temperature under an Ar atmosphere. Finally, the reactor temperature was raised to 700°C at a constant heating rate of $10^\circ\text{C}/\text{min}$ under a flow of H_2 (10%)/Ar (50 mL/min). The H_2 consumption was monitored by a thermal conductivity detector (TCD) during the experiment. The curve data of temperature programmed desorption of ammonia (NH_3 -TPD) were recorded by a thermal conductivity detector (TCD) in a Tianjin XQ TP5080 auto-adsorption apparatus. First, the quartz tube is added to the catalysts and a helium gas of 30 mL/min was introduced and the temperature of the furnace was raised from room temperature to 200°C with a $10^\circ\text{C}/\text{min}$ heating rate. After a span of 30 min at 200°C , the catalysts were cooling to 80°C . The sample was adsorbed for 30 min under pure ammonia gas conditions of 30 mL/min. The physically adsorbed ammonia to the surface of the catalyst was then purged with 30 mL/min helium for 1 h. At last, the catalysts were heated to 500°C at a heating rate of $5^\circ\text{C}/\text{min}$ under a helium gas flow of 30 mL/min, and a temperature-programmed ammonia desorption curve was recorded.

3.3. Catalyst Activity Evaluation

The device was used for NH_3 -SCR reaction activity evaluation process as shown in Figure 11. The catalytic activities of solid samples were evaluated in a fixedbed stainless steel micro-reactor loaded with 0.10 g of catalyst powder in 20 mesh size. The electrically heated wire and thermocouple in a fixedbed stainless steel micro-reactor was used to heat the mixed gas. In order to simulate the realistic exhaust condition, the composition of NH_3 , NO and O_2 in the feed gas were 0.12%, 0.10% and 3.60%, respectively. The total flow rate was 1.00 L/min and the gas hourly space velocity (GHSV) was 5000 h^{-1} . N_2 was used as balance gas and NH_3 was used as reductant. Catalytic activity was measured in a steady flow mode in a fixedbed stainless steel micro-reactor. Each part of gas was controlled by mass flow controllers. Prior to each activity test, the catalysts were pretreated at 200°C for 2 h with flowing air, and cooled to the initial reaction temperature around 100°C . The steady-state deNO_x activity test was then conducted in the reaction temperature range from 100 to 350°C at intervals of 50°C . Each temperature point was kept for 30 min to achieve a balanced reaction gas concentration and all of the data were obtained when the SCR reaction reached the steady state.

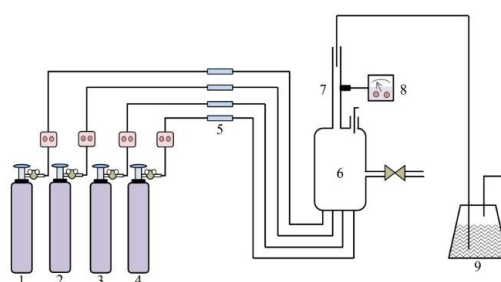


Figure 11. Flow chart of NH_3 -SCR reactivity evaluation. 1. N_2 2. O_2 3. NO 4. NH_3 5. Mass flow controllers 6. Gas generating system 7. Fixedbed stainless steel micro-reactor 8. The flue gas analyzer 9. Adsorbent.

An FT-IR gas analyzer (GASM ET DX 4000, Finland) was used for the purpose of analyzing the concentrations of NO_x (NO + NO₂) and N₂O in the outlet gas. The following Equations (1) and (2) were used to estimate the NO_x conversion and N₂ selectivity:

$$\text{NO conversion (\%)} = \frac{\text{NO}_{\text{in}} - \text{NO}_{\text{xout}}}{\text{NO}_{\text{in}}} \times 100\% \quad (1)$$

$$\text{N}_2 \text{ selectivity (\%)} = \frac{\text{NO}_{\text{in}} - \text{NO}_{\text{xout}} - 2\text{N}_2\text{O}_{\text{out}}}{\text{NO}_{\text{in}} - \text{NO}_{\text{xout}}} \times 100\% \quad (2)$$

where NO_{in} refers to the concentration of nitric oxide at the inlet of the reactor, NO_{xout} refers to the concentration of NO_x (NO + NO₂) at the outlet of the reactor, N₂O_{out} refers to the concentration of N₂O at the outlet of the reactor.

The catalytic activity experiments were done in triplicate. If the experimental data fluctuated greatly, it was discarded. If the fluctuation of the experimental data was less than 10%, it was averaged. Finally, the average was plotted in the figures. The error bar was plotted in the figures, which was used as an index to evaluate the difference between the average and measurement. The following Equations (3) and (4) were the experiment result average and error bar, respectively.

$$N_a = \frac{N_1 + N_2 + N_3}{3} \quad (3)$$

$$\text{Error bar} = \frac{\sum_{i=1}^3 |N_i - N_a|}{3} \quad (4)$$

where N_a represents the average of three experiment results, N₁, N₂ and N₃ represent the result of three experiments, respectively. N_i and N_a represent the measured and averaged result, respectively.

4. Conclusions

In this paper, an impregnation method was used to prepare the low-temperature SCR catalysts made of MnO_x-Cu loaded on activated carbon. Then, the catalysts were packed into the fixed bed reactor to evaluate the selective catalytic reduction of NO performance. The experimental results show that NO conversion is highest at 96.82% and it remains rather stable with a slight fluctuation around ±1% over time throughout the 25 h continuous procedure when the calcination temperature is 350 °C, and MnO_x loading amount is 5%, and Cu loading amount is 3%, and reaction temperature is 200 °C, which can meet the needs of deNO_x at a low temperature and provide reference for industrial production and application. The concentration of N₂O as a by-product in the outlet gas is measured. The results show that the concentration of N₂O is very low in the outlet gas of the reactor in the SCR reaction, and the selectivity to N₂ is almost 99%. Although much progress has been made in this research, many problems need to be solved. As for the development of low-temperature SCR catalysts in the future, it is worthwhile to explore Mn-based catalysts with excellent resistance to sulfur, water and so on. Discovering new doping elements and novel supports may be promising research directions, and monolithic catalysts should be given more consideration from a commercial perspective.

Author Contributions: All authors have contributed in various degrees to the analytical methods used, to the research concept, to the experiment design, to the acquisition of data, or analysis and interpretation of data, to draft the manuscript or to revise it critically for important intellectual content. All authors have read and agreed to the published version of the manuscript.

Funding: This research was funded by the Open Foundation of Shaanxi Key Laboratory of Lacustrine Shale Gas Accumulation and Exploitation (under planning), and the Major Science and Technology Projects of Shanxi Province (No.20181102017), and the Fundamental Research Funds for the Central Universities (No.2009QH03).

Acknowledgments: In this section you can acknowledge any support given which is not covered by the author contribution or funding sections. This may include administrative and technical support, or donations in kind (e.g., materials used for experiments).

Conflicts of Interest: The authors confirm that this article content contains no conflicts of interest.

References

1. Tang, C.J.; Zhang, H.L.; Dong, L. Ceria-based catalysts for low-temperature selective catalytic reduction of NO with NH₃. *Catal. Sci. Technol.* **2016**, *6*, 1248–1264. [[CrossRef](#)]
2. Mosrati, J.; Atia, H.; Eckelt, R.; Lund, H.; Agostini, G.; Bentrup, U.; Rockstroh, N.; Keller, S.; Armbruster, U.; Mhamdi, M. Nb-Modified Ce/Ti Oxide Catalyst for the Selective Catalytic Reduction of NO with NH₃ at Low Temperature. *Catalysts* **2018**, *8*, 175. [[CrossRef](#)]
3. Daood, S.S.; Yelland, T.S.; Nimmo, W. Selective non-catalytic reduction Fe-based additive hybrid technology. *Fule* **2017**, *208*, 353–362. [[CrossRef](#)]
4. Yan, Q.H.; Yang, R.Y.; Zhang, Y.L.; Umar, A.; Huang, Z.G.; Wang, Q. A comprehensive review on selective catalytic reduction catalysts for NO_x emission abatement from municipal solid waste incinerators. *Environ. Prog. Sustain.* **2016**, *35*, 1061–1069. [[CrossRef](#)]
5. Yang, G.; Zhao, H.T.; Luo, X.; Shi, K.Q.; Zhao, H.B.; Wang, W.K.; Chen, Q.H.; Fan, H.; Wu, T. Promotion effect and mechanism of the addition of Mo on the enhanced low temperature SCR of NO_x by NH₃ over MnO_x/gamma-Al₂O₃ catalysts. *Appl. Catal. B Environ.* **2019**, *245*, 743–752. [[CrossRef](#)]
6. Sala, R.; Dzida, J.; Krasowski, J. Ammonia Concentration Distribution Measurements on Selective Catalytic Reduction Catalysts. *Catalysts* **2018**, *8*, 231. [[CrossRef](#)]
7. Zhang, K.; Yu, F.; Zhu, M.Y.; Dan, J.M.; Wang, X.G.; Zhang, J.L.; Dai, B. Enhanced Low Temperature NO Reduction Performance via MnO_x-Fe₂O₃-Vermiculite Monolithic Honeycomb Catalysts. *Catalysts* **2018**, *8*, 100. [[CrossRef](#)]
8. Wang, R.H.; Hao, Z.F.; Li, Y.; Liu, G.Q.; Zhang, H.; Wang, H.T.; Xia, Y.G.; Zhan, S.H. Relationship between structure and performance of a novel highly dispersed MnO_x on Co-Al layered double oxide for low temperature NH₃-SCR. *Appl. Catal. B Environ.* **2019**, *258*, 983–992. [[CrossRef](#)]
9. Han, L.P.; Gao, M.; Hasegawa, J.; Li, S.X.; Shen, Y.J.; Li, H.R.; Shi, L.Y.; Zhang, D.S. SO₂-tolerant selective catalytic reduction of NO_x over meso-TiO₂@Fe₂O₃@Al₂O₃ metal-based monolith catalysts. *Environ. Sci. Technol.* **2019**, *53*, 6462–6473. [[CrossRef](#)]
10. Blanco, J.; Avila, P.; Suárez, S.; Yates, M.; Martin, J.A.; Marzo, L.; Knapp, C. CuO/NiO monolithic catalysts for NO_x removal from nitric acid plant flue gas. *Chem. Eng. J.* **2004**, *97*, 1–9. [[CrossRef](#)]
11. Lin, T.; Zhang, Q.L.; Li, W.; Gong, M.C.; Xing, Y.X.; Chen, Y.Q. Monolith Manganese-Based Catalyst Supported on ZrO₂-TiO₂ for NH₃-SCR Reaction at Low Temperature. *Acta Phys. Chim. Sin.* **2008**, *24*, 1127–1131. [[CrossRef](#)]
12. Brookshear, D.W.; Nam, J.; Nguyen, K.; Toops, T.J.; Binder, A. Impact of sulfation and desulfation on NO_x reduction using Cu-chabazite SCR catalysts. *Catal. Today* **2015**, *258*, 359–366. [[CrossRef](#)]
13. Xiao, X.; Sheng, Z.; Yang, L.; Dong, F. Low-temperature selective catalytic reduction of NO_x with NH₃ over a manganese and cerium oxide/graphene composite prepared by a hydrothermal method. *Catal. Sci. Technol.* **2016**, *6*, 1507–1514. [[CrossRef](#)]
14. Chmielarz, L.; Kuśtrowski, P.; Rafalskalasocha, A.; Majda, D.; Dziembaj, R. Catalytic activity of Co-Mg-Al, Cu-Mg-Al and Cu-Co-Mg-Al mixed oxides derived from hydrotalcites in SCR of NO with ammonia. *Appl. Catal. B Environ.* **2002**, *35*, 195–210. [[CrossRef](#)]
15. Wan, Y.; Zhao, W.; Tang, Y.; Li, L.; Wang, H.J.; Cui, Y.L.; Gu, J.L.; Li, Y.S.; Shi, J.L. Ni-Mn bi-metal oxide catalysts for the low temperature SCR removal of NO with NH₃. *Appl. Catal. B Environ.* **2014**, *148*, 114–122. [[CrossRef](#)]
16. Thirupathi, B.; Smirniotis, P.G. Nickel-doped Mn/TiO₂ as an efficient catalyst for the low-temperature SCR of NO with NH₃: Catalytic evaluation and characterizations. *J. Catal.* **2012**, *288*, 74–83. [[CrossRef](#)]
17. Qi, G.S.; Yang, R.T. Performance and kinetics study for low-temperature SCR of NO with NH₃ over MnO_x-CeO₂ catalyst. *J. Catal.* **2003**, *217*, 434–441. [[CrossRef](#)]
18. Ouzzine, M.; Cifredo, G.A.; Gatica, J.M.; Harti, S.; Chafik, T.; Vidal, H. Original carbon-based honeycomb monoliths as support of Cu or Mn catalysts for low-temperature SCR of NO: Effects of preparation variables. *Appl. Catal. A Gen.* **2008**, *342*, 150–158. [[CrossRef](#)]
19. Yao, X.; Kong, T.; Chen, L.; Ding, S.; Yang, F.; Dong, L. Enhanced low-temperature NH₃-SCR performance of MnO_x/CeO₂ catalysts by optimal solvent effect. *Appl. Surf. Sci.* **2017**, *420*, 407–415. [[CrossRef](#)]
20. Gao, C.; Shi, J.W.; Fan, Z.Y.; Gao, G.; Niu, C.M. Sulfur and Water Resistance of Mn-Based Catalysts for Low-Temperature Selective Catalytic Reduction of NO_x: A Review. *Catalysts* **2018**, *8*, 11. [[CrossRef](#)]

21. Wang, P.C.; Yao, L.; Pu, Y.J.; Yang, L.; Jiang, X.; Jiang, W.J. Low-temperature selective catalytic reduction of NO_x with NH₃ over an activated carbon-carbon nanotube composite material prepared by in situ method. *RSC Adv.* **2019**, *9*, 36658–36663. [[CrossRef](#)]
22. Liu, K.J.; Yu, Q.B.; Wang, B.L.; Qin, Q.; Wei, M.Q.; Fu, Q. Low temperature selective catalytic reduction of nitric oxide with urea over activated carbon supported metal oxide catalysts. *Environ. Technol.* **2018**, 1–14. [[CrossRef](#)] [[PubMed](#)]
23. Huang, L.H.; Li, X.; Chen, Y.Q. The effect of the oxidation method of an activated carbon on the selective catalytic reduction of NO_x with NH₃ over CeO₂/activated carbon catalysts. *New Carbon Mater.* **2018**, *33*, 237–244.
24. Samojeden, B.; Grzybek, T. The influence of the promotion of N-modified activated carbon with iron on NO removal by NH₃-SCR (Selective catalytic reduction). *Energy* **2016**, *116*, 1484–1491. [[CrossRef](#)]
25. Li, Y.R.; Guo, Y.Y.; Xiong, J.; Zhu, T.Y.; Hao, J.K. The Roles of Sulfur-Containing Species in the Selective Catalytic Reduction of NO with NH₃ over Activated Carbon. *Ind. Eng. Chem. Res.* **2016**, *55*, 12341–12349. [[CrossRef](#)]
26. Valdés-Sols, T.; Marbán, G.; Fuertes, A.B. Low-temperature SCR of NO_x with NH₃ over carbon-ceramic supported catalysts. *Appl. Catal. B Environ.* **2003**, *46*, 261–271. [[CrossRef](#)]
27. García-bordejé, E.; Calvillo, L.; Lázaro, M.J.; Moliner, R. Vanadium supported on carbon-coated monoliths for the SCR of NO at low temperature: Effect of pore structure. *Appl. Catal. B Environ.* **2004**, *50*, 235–242. [[CrossRef](#)]
28. Wang, Y.L.; Huang, Z.G.; Liu, Z.Y.; Liu, Q.Y. A novel activated carbon honeycomb catalyst for simultaneous SO₂ and NO removal at low temperatures. *Carbon* **2004**, *42*, 423–460. [[CrossRef](#)]
29. Zhu, Z.P.; Liu, Z.Y.; Niu, H.X.; Liu, S.J.; Hu, T.D.; Liu, T.; Xie, Y.N. Mechanism of SO₂ Promotion for NO Reduction with NH₃ over Activated Carbon-Supported Vanadium Oxide Catalyst. *J. Catal.* **2001**, *197*, 6–16. [[CrossRef](#)]
30. Ye, T.; Chen, D.L.; Yin, Y.S.; Liu, J.; Zeng, X. Experimental Research of an Active Solution for Modeling In Situ Activating Selective Catalytic Reduction Catalyst. *Catalysts* **2018**, *7*, 258. [[CrossRef](#)]
31. Flura, A.; Can, F.; Courtois, X.; Royer, S.; Duprez, D. High-surface-area zinc aluminate supported silver catalysts for low-temperature SCR of NO with ethanol. *Appl. Catal. B Environ.* **2012**, *126*, 275–289. [[CrossRef](#)]
32. Zhao, S.; Huang, L.M.; Jiang, B.Q.; Cheng, M.; Zhang, J.W.; Hu, Y.J. Stability of Cu-Mn bimetal catalysts based on different zeolites for NO_x removal from diesel engine exhaust. *Chin. J. Catal.* **2018**, *39*, 800–809. [[CrossRef](#)]
33. Jiang, H.X.; Zhao, J.; Jiang, D.Y.; Zhang, M.H. Hollow MnO_x-CeO₂ nanospheres prepared by a green route: A novel low-temperature NH₃-SCR catalyst. *Catal. Lett.* **2014**, *144*, 325–332. [[CrossRef](#)]
34. Xu, L.T.; Niu, S.L.; Lu, C.M.; Zhang, Q.; Li, J. Influence of calcination temperature on Fe_{0.8}Mg_{0.2}O_z catalyst for selective catalytic reduction of NO_x with NH₃. *Fuel* **2018**, *219*, 248–258. [[CrossRef](#)]
35. Huang, L.; Zong, Y.H.; Wang, H.; Li, Q.; Chen, T.; Dong, L.; Zou, W.X.; Guo, K. Influence of calcination temperature on the plate-type V₂O₅-MoO₃/TiO₂ catalyst for selective catalytic reduction of NO. *React. Kinet. Mech. Catal.* **2018**, *124*, 603–617. [[CrossRef](#)]
36. Ren, B.N. Low-temperature selective catalytic reduction of NO with NH₃ over CuO_x/CNTs Catalyst. *Mat. Sci. Eng. R.* **2017**, *281*, 12006. [[CrossRef](#)]
37. Jiang, L.J.; Liu, Q.C.; Zhao, Q.; Ren, S.; Kong, M.; Yao, L.; Meng, F. Promotional effect of Ce on the SCR of NO with NH₃ at low temperature over MnO_x supported by nitric acid-modified activated carbon. *Res. Chem. Intermed.* **2018**, *44*, 1729–1744. [[CrossRef](#)]
38. Tang, X.L.; Hao, J.M.; Xu, W.G.; Li, J.H. Low temperature selective catalytic reduction of NO_x with NH₃ over amorphous MnO_x catalysts prepared by three methods. *Catal. Commun.* **2006**, *8*, 329–334. [[CrossRef](#)]
39. Wang, T.; Zhang, X.Y.; Liu, J.; Liu, H.Z.; Wang, Y.; Sun, B.M. Effects of temperature on NO_x removal with Mn-Cu/ZSM5 catalysts assisted by plasma. *Appl. Therm. Eng.* **2018**, *130*, 1224–1232. [[CrossRef](#)]
40. Gao, X.; Liu, S.J.; Zhang, Y.; Luo, Z.Y.; Cen, K.F. Physicochemical properties of metal-doped activated carbons and relationship with their performance in the removal of SO₂ and NO. *J. Hazard. Mater.* **2011**, *188*, 58–66. [[CrossRef](#)]
41. Xin, Y.; Li, H.; Zhang, N.N.; Li, Q.; Zhang, Z.L.; Cao, X.M.; Hu, P.; Zheng, L.R.; Anderson, J.A. Molecular-level insight into selective catalytic reduction of NO_x with NH₃ to N₂ over a highly efficient bifunctional V- α -MnO_x catalyst at low temperature. *ACS Catal.* **2018**, *8*, 4937–4949. [[CrossRef](#)]

42. Yao, Z.; Guo, Y.X.; Yang, Y.J.; Huang, H.; Qu, D.L. MnO_x-CeO_x Nanoparticles supported on graphene aerogel for selective catalytic reduction of nitric oxides. *J. Nanomater.* **2019**, 4239764. [[CrossRef](#)]
43. Lee, S.M.; Park, K.H.; Hong, S.C. MnO_x/CeO₂-TiO₂ mixed oxide catalysts for the selective catalytic reduction of NO with NH₃ at low temperature. *Chem. Eng. J.* **2012**, *195*, 323–331. [[CrossRef](#)]
44. Fang, D.; Xie, J.L.; Mei, D.; Zhang, Y.M.; He, F.; Liu, X.Q.; Li, Y.M. Effect of CuMn₂O₄ spinel in Cu–Mn oxide catalysts on selective catalytic reduction of NO_x with NH₃ at low temperature. *RSC Adv.* **2014**, *4*, 25540–25551. [[CrossRef](#)]
45. Zhang, M.H.; Cao, H.B.; Chen, Y.F.; Jiang, H.X. Role of Mn: Promotion of Fast-SCR for Cu-SAPO-34 in Low-Temperature Selective Catalytic Reduction with Ammonia. *Catal. Surv. Asia* **2019**, *23*, 245–255. [[CrossRef](#)]
46. Cai, S.X.; Zhang, D.S.; Zhang, L.; Huang, L.; Li, H.R.; Gao, R.H.; Shi, L.Y.; Zhang, J.P. Comparative study of 3D ordered macroporous Ce_{0.75}Zr_{0.2}M_{0.05}O₂-delta (M = Fe, Cu, Mn, Co) for selective catalytic reduction of NO with NH₃. *Catal. Sci. Technol.* **2014**, *4*, 93–101. [[CrossRef](#)]
47. Shen, Q.; Zhang, L.Y.; Sun, N.N.; Wang, H.; Zhong, L.S.; He, C.; Wei, W.; Sun, Y.H. Hollow MnO_x-CeO₂ mixed oxides as highly efficient catalysts in NO oxidation. *Chem. Eng. J.* **2017**, *322*, 46–55. [[CrossRef](#)]
48. Yao, Z.; Qu, D.L.; Guo, Y.X.; Yang, Y.J.; Huang, H. Fabrication and Characteristics of Mn@ Cu₃(BTC)₂ for Low-Temperature Catalytic Reduction of NO_x with NH₃. *Adv. Mater. Sci. Eng.* **2019**, *2019*, 2935942. [[CrossRef](#)]
49. Shu, Y.; Zhang, F.; Wang, H.C. Manganese-cerium mixed oxides supported on rice husk based activated carbon with high sulfur tolerance for low-temperature selective catalytic reduction of nitrogen oxides with ammonia. *RSC Adv.* **2019**, *9*, 23964–23972. [[CrossRef](#)]
50. Yu, C.L.; Chen, F.; Dong, L.F.; Liu, X.Q.; Huang, B.C.; Wang, X.N.; Zhong, S.B. Manganese-rich MnSAPO-34 molecular sieves as an efficient catalyst for the selective catalytic reduction of NO_x with NH₃: One-pot synthesis, catalytic performance, and characterization. *Environ. Sci. Pollut. R.* **2017**, *24*, 7499–7510. [[CrossRef](#)]
51. Luo, S.P.; Zhou, W.T.; Xie, A.J.; Wu, F.Q.; Yao, C.; Li, X.Z.; Zuo, S.X.; Liu, T.H. Effect of MnO₂ polymorphs structure on the selective catalytic reduction of NO_x with NH₃ over TiO₂-Palygorskite. *Chem. Eng. J.* **2016**, *286*, 291–299. [[CrossRef](#)]
52. Yan, Q.H.; Chen, S.N.; Zhang, C.; O'Hare, D.; Wang, Q. Synthesis of Cu_{0.5}Mg_{1.5}Mn_{0.5}Al_{0.5}O_x mixed oxide from layered double hydroxide precursor as highly efficient catalyst for low-temperature selective catalytic reduction of NO_x with NH₃. *J. Colloid Interf. Sci.* **2018**, *526*, 63–74. [[CrossRef](#)]
53. Bennici, S.; Carniti, P.; Gervasini, A. Bulk and surface properties of dispersed CuO phases in relation with activity of NO_x reduction. *Catal. Lett.* **2004**, *98*, 187–194. [[CrossRef](#)]
54. Dong, G.J.; Li, Y.M.; Wang, Y.G.; Zhang, J.; Duan, R.R. DeNO_x performance of Cu-Mn composite catalysts prepared by the slurry coating method. *React. Kinet. Mech. Cat.* **2014**, *111*, 235–245. [[CrossRef](#)]
55. Yan, Q.H.; Gao, Y.S.; Li, Y.R.; Vasiliades, M.A.; Chen, S.N.; Zhang, C.; Gui, R.R.; Wang, Q.; Zhu, T.Y.; Efstathiou, A.M. Promotional effect of Ce doping in Cu₄Al₁O_x-LDO catalyst for low-T practical NH₃-SCR: Steady-state and transient kinetics studies. *Appl. Catal. B Environ.* **2019**, *255*, 117749. [[CrossRef](#)]
56. Zhu, B.Z.; Li, G.B.; Sun, Y.L.; Yin, S.L.; Fang, Q.L.; Zi, Z.H.; Zhu, Z.C.; Li, J.X.; Mao, K.K. De-NO_x Performance and Mechanism of Mn-Based Low-Temperature SCR Catalysts Supported on Foamed Metal Nickel. *J. Brazil. Chem. Soc.* **2018**, *29*, 1680–1689. [[CrossRef](#)]
57. Efstathiou, A.M.; Fliatoura, K. Selective catalytic reduction of nitric oxide with ammonia over V₂O₅/TiO₂ catalyst: A steady-state and transient kinetic study. *Appl. Catal. B Environ.* **1995**, *6*, 35–59. [[CrossRef](#)]
58. Stathopoulos, V.N.; Belessi, V.C.; Costa, C.N.; Neophytides, S.; Falaras, P.; Efstathiou, A.M.; Pomonis, P.J. Catalytic activity of high surface area mesoporous Mn-based mixed oxides for the deep oxidation of methane and lean-NO_x reduction. *Stud. Surf. Sci. Catal.* **2000**, *130*, 1529–1534.
59. Damma, D.; Ettireddy, P.R.; Reddy, B.M.; Smirniotis, P.G. A Review of Low Temperature NH₃-SCR for Removal of NO_x. *Catalysts* **2019**, *9*, 349. [[CrossRef](#)]
60. Wang, J.H.; Zhao, H.W.; Haller, G.; Li, Y.D. Recent advances in the selective catalytic reduction of NO_x with NH₃ on Cu-Chabazite catalysts. *Appl. Catal. B Environ.* **2017**, *202*, 346–354. [[CrossRef](#)]
61. Gao, F.; Peden, C.H.F. Recent Progress in Atomic-Level Understanding of Cu/SSZ-13 Selective Catalytic Reduction Catalysts. *Catalysts* **2018**, *8*, 140.

62. Wang, S.X.; Guo, R.T.; Pan, W.G.; Chen, Q.L.; Sun, P.; Li, M.Y.; Liu, S.M. The deactivation of Ce/TiO₂ catalyst for NH₃-SCR reaction by alkali metals: TPD and DRIFT studies. *Catal. Commun.* **2017**, *89*, 143–147. [[CrossRef](#)]
63. Kijlstra, W.S.; Brands, D.S.; Poels, E.K.; Blik, A. Kinetics of the selective catalytic reduction of NO with NH₃ over MnO_x/Al₂O₃ catalysts at low temperature. *Catal. Today* **1999**, *50*, 133–140. [[CrossRef](#)]
64. Park, K.H.; Lee, S.M.; Kim, S.S.; Kwon, D.W.; Hong, S.C. Reversibility of Mn Valence State in MnO_x/TiO₂ Catalysts for Low-temperature Selective Catalytic Reduction for NO with NH₃. *Catal. Lett.* **2013**, *143*, 246–253. [[CrossRef](#)]
65. Li, J.H.; Chang, H.Z.; Ma, L.; Hao, J.M.; Yang, R.T. Low-temperature selective catalytic reduction of NO_x with NH₃ over metal oxide and zeolite catalysts—A review. *Catal. Today* **2011**, *175*, 147–156. [[CrossRef](#)]
66. Yang, Y.J.; Liu, J.; Liu, F.; Wang, Z.; Ding, J.Y.; Huang, H. Reaction mechanism for NH₃-SCR of NO_x over CuMn₂O₄ catalyst. *Chem. Eng. J.* **2019**, *361*, 578–587. [[CrossRef](#)]



© 2020 by the authors. Licensee MDPI, Basel, Switzerland. This article is an open access article distributed under the terms and conditions of the Creative Commons Attribution (CC BY) license (<http://creativecommons.org/licenses/by/4.0/>).